Controlled Synthesis of Co_3O_4 Nanoparticles through Oriented Aggregation

Tao He, Dairong Chen,* and Xiuling Jiao

Department of Chemistry, Shandong University, Jinan 250100, People's Republic of China

Received March 25, 2003. Revised Manuscript Received November 26, 2003

Monodispersed 5-nm Co_3O_4 nanocrystals are prepared by thermal decomposition, in long carbon chain alcohols, of the intermediate product $Co(NO_3)_2 \cdot 7C_6H_{13}OH$, which is first obtained through the reaction of $Co(NO_3)_2 \cdot 6H_2O$ with *n*-hexanol. A designed addition of water into the reaction system causes an oriented aggregation of the primary nanocrystals resulting in spherical mesoporous-like nanostructures from tens to several hundred nanometers. IR, XRD, UV−visible, and ^1H NMR analysis techniques are applied to determine the intermediate product, and the thermal-decomposition mechanism is identified through gas chromatography-mass spectrum analysis. XRD, TEM, HRTEM, SAED, and TG/MS are used to characterize the oriented aggregating nanostructures. The binder effect of water molecules on the oriented aggregation of the building blocks and the capping effect of the alcohols on the particle surface during the process are discussed.

Introduction

One of the main goals of nanomaterial synthesis is the creation of monodispersed nanoparticles with controlled size. This guarantees identical physical and chemical properties and makes the investigation of the relations between the properties and particle sizes possible. The construction of uniform nanoparticles as building blocks has been extensively investigated for the self-assembly of two- and three-dimensional superlattices aimed at constructing novel nanodevices. Further, monodispersed nanoparticles as the ideal raw materials for ceramic sintering, pigments, magnetic fluids, and many other dispersion systems has also been studied. However, a small amount of work is reported on the preparation of monodispersed transition metal oxide nanoparticles with controlled size compared with that of the non-oxide nanoparticles. In the last 2 decades, the precipitation from the homogeneous electrolyte solution has been intensively investigated, and a great deal of metal oxide colloid particles in submicro- to micrometer scales is now prepared through this method.[1] Additionally, solution-phase chemical routes have also been used for preparing monodispersed metal oxide nanoparticles.[2−8] When metal alkoxides are used as the raw materials, the hydrolysis and polycondensation (nucleation and growth) can be controlled by adjusting the reaction conditions to prepare the monodispersed nanoparticles.[2] Particle size can also be controlled by quenching the growth of the formed crystal nuclei by means of adding capping ligands into the homogeneous solution.[3,4] Similarly, microemulsions, inverse micelles, and copolymers can provide separate microreactors where the nucleation and growth of metal oxides are confined to control particle size.[5−7] In addition, there are some other methods such as the sol−gel process and hydrothermal process and so forth applied in the domains.[8] To prepare nanocrystal oxides without hydroxyl on the particle surface, thermodecomposition of organometallics that has been assisted by organic capping ligands in non-hydrolytic solution is studied, and a series of monodispersed metal oxide nanocrystals have been successfully obtained.[4]

The nucleation of oxide crystals is usually too fast in solution. Control over the subsequent growth step appears much more feasible. Aggregation[9−18] and coars-

* To whom correspondence should be addressed. Phone: +86-531-8364280. E-mail: cdr@sdu.edu.cn.

(1) Matijević, E. *Chem. Mater.* **1993**, *5*, 412.
(2) Moritz, T.; Reiss, J.; Diesner, K.; Su, D.; Chemseddine, A. *J. Phys. Chem. B* **1997**, *101*, 8052.
(3) (a)Yin, J. S.; Wang, Z. L. *J. Phys. Chem. B* **1997**, *101*, 8979. (b) Brock, S. L.; Sanabria, M.; Suib, S. L. *J. Phys. Chem. B* **1999**, *103*, 7416. (c) Wong, E. M.; Hoertz, P. G.; Liang, C. J.; Shi, B.-M.; Meyer, G. J.; Searson, P. C. *Langmuir* **2001**, *17*, 8362. (d) Pesika, N. S.; Hu, Z.; Stebe, K. J.; Searson, P. C. *J. Phys. Chem. B* **2002**, *106*, 6985.
(4) (a) Trentler, T. J.; Denler, T. E.; Bertone, J. F.; Agrawal, A.; Colvin, V. L. *J. Am. Chem. Soc.* **1999**, *121*, 1613. (b) Rockenberger, J.; Scher, E. C.; Alivisatos, A. P. *J. Am. Chem. Soc.* **1999**, *121*, 11595. (c) Hyeon, T.; Lee, S. S.; Park, J.; Chung, Y.; Na, H. B. *J. Am. Chem. Soc.* **2001**, *123*, 12798. (d) Sun, S.; Zeng, H. *J. Am. Chem. Soc.* **2002**, *124*, 8204. (e) Guo, Q.; Teng, X.; Rahman, S.; Yang, H. *J. Am. Chem. Soc.* **2003**, *125*, 630.
(5) (a) Moumen, N.; Pileni, M. P. *J. Phys. Chem.* **1996**, *100*, 1867. (b) Zhang, J.; Ju, X.; Wu, Z. Y.; Liu, T.; Hu, T. D.; Xie, Y. N. *Chem. Mater.* **2001**, *13*, 4192. (c) Vestal, C. R.; Zhang, Z. J. *Chem. Mater.* **2002**, *14*, 3817.
(6) O'Brien, S.; Brus, L.; Murray, C. B. *J. Am. Chem. Soc.* **2001**, *123*, 12085.
(7) (a) Underhill, R. S.; Liu, G. *Chem. Mater.* **2000**, *12*, 2082. (b) Ahmed, S. R.; Kofinas, P. *Macromolecules* **2002**, *35*, 3338.
(8) (a) Wu, N.-L.; Wang, S.-Y.; Rusakova, I. A. *Science* **1999**, *285*, 1375. (b) Liu, C.; Zou, B.; Rondinone, A. J.; Zhang, Z. J. *J. Am. Chem. Soc.* **2001**, *123*, 4344. (c) Niederberger, M.; Krumeich, F.; Hegetschweiler, K.; Nesper, R. *Chem. Mater.* **2002**, *14*, 78.
(9) (a) Hsu, W. P.; Ronnquist, L.; Matijević, E. *Lungmuir* **1988**, *4*, 31. (c) Ocaña, M.; Matijević, E. *J. Mater. Res.* **1990**, *5*, 1083. (d) Ocaña, M.; Serna, C. J.; Matijević, E. *Mater. Lett.* **1991**, *12*, 32. (e) Morales, M. P.; Gonzáles, C. T.; Serna, C. J. *J. Mater. Res.* **1992**, *7*, 2538.
(10) Bailey, J. K.; Brinker, C. J.; Mecartney, M. L *J. Colloid. Interface Sci.* **1993**, *157*, 1.
(11) (a) Penn, R. L.; Banfield, J. F. *Am. Mineral.* **1998**, *83*, 1077. (b) Penn, R. L.; Banfield, J. F. *Science* **1998**, *281*, 969. (c) Penn, R. L.; Banfield, J. F. *Geochim. Cosmochim. Acta* **1999**, *63*, 1549. (d) Penn, R. L.; Banfield, J. F. *Am. Mineral.* **1999**, *84*, 871.

10.1021/cm0303033 CCC: $27.50
Published on Web 01/21/2004

ening[19] have been found as the two main competitive growth modes of nanoparticles. This is especially evident in aqueous solutions. Coarsening[19] (known as Ostwald ripening) is the growth of larger crystals at the expense of smaller crystals. The aggregation of nanocrystals often leads to polycrystalline solids.[18] Single (nanometer sized) crystals can also be formed through the oriented aggregation of nanocrystals or nanoclusters.[10−16] Oriented aggregation is a recent discovery and attracts much attention as a promising method for creating advanced artificial materials with distinct micro- and nanostructures and as clues for the explanation of the defects formation in crystal growth.[11,14] The oriented aggregation phenomena of several metal oxides have been investigated in detail, providing another potential method for the control over microstructures, morphologies, and particle size.[16,17]

In the literature, investigations have focused on the aggregation of primary particles in aqueous solutions. The present paper introduces a novel method for aggregating oriented nanocrystals in nonaqueous (long carbon chain alcohols) solutions that produces monodispersed particles with a controlled particle size from tens to several hundred nanometers. Five-nanometer Co_3O_4 nanocrystals (capped by the long carbon chain alcohol and monodispersed in hydrocarbons) form in the system and then aggregate to oriented larger particles when a small amount of water is added. Compared with the aggregation process in aqueous solution, the particle size is easily controlled by the variation of the molar ratio of H_2O to metal ions. It is well-known that surface hydroxyls are the main reason for the aggregation of metal oxide nanoparticles,[20] and thus water in the process actually acts as a binder, controlling the nanocrystal aggregation. Compared with the fast nucleation and aggregation growth in aqueous solution, it is thought that nanocrystals aggregating in the nonaqueous solution are kinetically slower due to less surface hydroxyls and greater viscosity. This is thought to give the nanocrystals enough cushion to rotate to find the low-energy configuration interface and form perfectly oriented aggregations in the formed nanoparticles.[14] Furthermore, the surface-capped nanocrystals, used herein as building blocks, apparently could not give compact single-crystal structure and a mesoporous-like structure is obtained.

The spinel structure Co_3O_4 is an important magnetic p-type semiconductor known by its applications in many fields such as heterogeneous catalysts,[21] anode material in Li-ion rechargeable batteries,[22] solid-state sensors,[23] electrochromic devices,[24] solar energy absorbers,[25] pigments,[26] and so on. To modify or promote its intrinsic properties, attention is focused on the preparation of the nanostructured Co_3O_4. This is achieved by pursuing a controlled surface area and porosity,[27] and distinct nanostructures including films, tubes, fibers, and rods.[28] The monodispersed 100-nm Co_3O_4 cubic nanocrystals were prepared through a forced hydrolysis method at relatively low temperature 23 years ago.[26] Recently, the 47-nm monodispersed Co_3O_4 cubic nanocrystals were obtained through the salt-solvent process.[29] Eight years ago 200−300-nm Co_3O_4 spherical particles formed by aggregation of much finer particles in homogeneous aqueous solutions were reported.[30] To the best of our knowledge, no other work has been done on the controlled synthesis of monodispersed Co_3O_4 nanoparticles. It is expected that this novel method of producing nanostructured oriented aggregates of the 5-nm nanocrystals will be interesting to others investigating the physical properties of the magnetic p-type semiconductor Co_3O_4. Furthermore, the large surface area caused by the mesopore and the various defects introduced by the oriented aggregation can promote their chemical activities and might give an impact to a certain extent to its applications.

Experimental Section

Synthesis. Experimental Apparatus. All the synthesis processes were carried out in a simple experimental apparatus exhibited in Figure 1.

Synthesis of the Intermediate Product. Five grams of $Co(NO_3)_2{\cdot}6H_2O$ was dissolved into 50.0 mL of *n*-hexanol to form a red solution and this solution was refluxed for 10 h at a reduced pressure (during the process, the boiling point continued increasing from 90 to 110 °C). And then about 30−40 mL of the superfluous solvent was distilled out. After the solution cooled to room temperature, a 15.0 g red solid crystallized.

Thermal Decomposition of the Intermediate Product to Nanocrystals. One and a half grams of red solid was

(12) Onuma, K.; Ito, A. *Chem. Mater.* **1998**, *10*, 3346.
(13) Privman, V.; Goia, D. V.; Park, J.; Matijević, E. J. *J. Colloid Interface Sci.* **1999**, *213*, 36.
(14) (a) Banfield, J. F.; Welch, S. A.; Zhang, H.; Ebert, T. T.; Penn, R. L. *Science* **2000**, *289*, 751. (b) Alivisatos, A. P. *Science* **2000**, *289*, 736.
(15) Penn, R. L.; Oskam, G.; Strathmann, T. J.; Searson, P. C.; Stone, A. T.; Veblen, D. R. *J. Phys. Chem. B* **2001**, *105*, 2177.
(16) Oskam, G.; Nellore, A.; Penn, R. L.; Searson, P. C. *J. Phys. Chem. B* **2003**, *107*, 1734.
(17) Pacholski, C.; Kornowski, A.; Weller, H. *Angew. Chem., Int. Ed.* **2002**, *41*, 1188.
(18) (a) Matijević, E. *Mater. Res. Soc. Bull.* **1989**, *14*, 18. (b) Park, J.; Privman, V.; Matijević, E. *J. Phys. Chem. B* **2001**, *105*, 11630. (c) Murphy-Wilhelmy, D.; Matijević, E. *J. Chem. Soc., Faraday Trans. 1* **1984**, *80*, 563. (d) Matijević, E.; Murphy-Wilhelmy, D. *J. Colloid Interface Sci.* **1982**, *86*, 476. (e) Matijević, E.; Scheiner, P. *J. Colloid Interface Sci.* **1978**, *63*, 509.
(19) Wong, E. M.; Bonevich, J. E.; Searson, P. C. *J. Phys. Chem. B* **1998**, *102*, 7770.
(20) (a) Brinker, C. E.; Scherer, G. W. *Sol−Gel Sci*; Academic Press: San Diego, CA, 1990; p 515. (b) Wu, N. L.; Wu, L. F.; Rusakova, I. A.; Hamed, A.; Litvinchuk, A. P. *J. Am. Ceram. Soc.* **1999**, *82*, 67.
(21) (a) Okamoto, Y.; Imanaka, T.; Teranishi, S. *J. Catal.* **1980**, *65*, 448. (b) Weichel, S.; Møller, P. *J. Surf. Sci.* **1998**, *399*, 219. (c) Nkeng, P.; Koening, J.; Gautier, J.; Chartier, P.; Poillerat, G. *J. Electroanal. Chem.* **1996**, *402*, 81.
(22) (a) Poizot, P.; Laruelle, S.; Grugeon, S.; Dupont, L.; Tarason, J.-M. *Nature* **2000**, *407*, 496. (b) Yuan, Z.; Huang, F.; Feng, C.; Sun, J.; Zhou, Y. *Mater. Chem. Phys.* **2002**, *9673*, 1.
(23) (a) Yamaura, H.; Tamaki, J.; Moriya, K.; Miura, N.; Yamazoe, N. *J. Electrochem. Soc.* **1997**, *144*, L158. (b) Ando, M.; Kobayashi, T.; Lijima, S.; Haruta, M. *J. Mater. Chem.* **1997**, *7*, 1779.
(24) (a) Svegl, F.; Orel, B.; Hutchins, M. G.; Kalcher, K. *J. Electrochem. Soc.* **1996**, *143*, 1532. (b) Maruyama, T.; Arai, S. *J. Electrochem. Soc.* **1996**, *143*, 1383.
(25) (a) Hutchins, M. G.; Wright, P. J.; Grebenik, P. D. *Solar Energy Mater.* **1987**, *16*, 113. (b) Ramachandram, K.; Oriakhi, C. O.; Lerner, M. M.; Koch, V. R. *Mater. Res. Bull.* **1996**, *31*, 767.
(26) Sugimoto, T.; Matijević, E. *J. Inorg. Nucl. Chem.* **1979**, *41*, 165.
(27) (a) Xu, Z. P.; Zeng, H. C. *J. Mater. Chem.* **1998**, *8*, 2499. (b) Xu, Z. P.; Zeng, H. C. *Chem. Mater.* **1999**, *11*, 67. (c) Xu, Z. P.; Zeng, H. C. *Chem. Mater.* **2000**, *12*, 3459.
(28) (a) Barreca, D.; Massignan, C. *Chem. Mater.* **2001**, *13*, 588. (b) Shi, X. S.; Han, S.; Sanedrin, R. J.; Zhou, F.; Selke, M. *Chem. Mater.* **2002**, *14*, 1897. (c) Lakshmi, B. B.; Patrissi, C. J.; Martin, C. R. *Chem. Mater.* **1997**, *9*, 2544. (d) Liu, Y.; Wang, G.; Xu, C.; Wang, W. *Chem. Commun.* **2002**, 1486.
(29) Xu, R.; Zeng, H. C. *J. Phys. Chem. B* **2003**, *107*, 926.
(30) Furlanetto, G.; Formaro, L. *J. Colloid Interface Sci.* **1995**, *170*, 169.

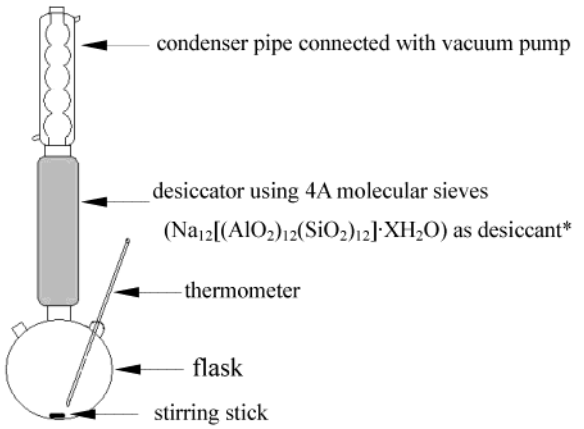

Figure 1. Illustration of the reaction apparatus. (*We note that the size of the water molecule (about 3 Å) is smaller than 4 Å and the size of the solvent molecule used here is much larger than 4 Å, for example, the size of *n*-hexyl alcohol is about 6 Å. Furthermore, the molecular sieves are known by their high drying efficiency even at high temperature and low fractional pressure conditions; thus, water can be completely separated from the reaction system with the current detection method such as IR spectroscopy.)

dissolved into 80 mL of absolute *n*-octanol, and the solution was refluxed at a reduced pressure for 3 h. Then the temperature was raised to 150 °C and kept for 0.5 h to form the final product. The monodispersed nanocrystals were separated by centrifugation and then washed with cyclohexane three times.

Controlled Synthesis of the Nanoparticles. One and half grams of intermediate was dissolved into 40 mL of absolute *n*-octanol in which a certain quantity of deionized water (40, 130, and 370 μL) was added to form a red solution, the solution was agitated magnetically at room temperature for 0.5 h, and then it was heated at 180 °C for 4 h to obtain the monodispersed nanoparticles.

Characterization

Structures of the products and the intermediates were studied using X-ray diffraction (XRD) on a Rigaku D/Max 2200-PC diffractometer with Cu Kα radiation ($\lambda = 0.15418$ nm) and graphite monochromator at ambient temperature. The surface properties of the nanocrystals and the intermediate product were characterized with a Nicolet 5DX FT-IR instrument using a KBr pellet technique. UV−visible (Perkin-Elmer spectrophotometer, Lamda 35) and ^{1}H nuclear magnetic resonance (Bruker AVANCE 600 M, ^{1}H NMR) techniques were used to characterize the coordination of Co^{2+} in the intermediate. Elemental analyses were done to identify the constituents of the intermediate product. Before the analysis, the sample was first leached drop by drop with cyclohexane and then dried in vacuum conditions at 30 °C to eliminate the solvent.

The decomposition mechanism of intermediate ($Co(NO_3)_2\cdot 7C_6H_{13}OH$) in alcohol solution was examined with the gas chromatography-mass spectrum analysis (Agilent 6890N-5973N GC/MSD). The supernatant fluid was separated for gas chromatography-mass spectrum analysis by centrifugation.

To substantiate the adhesive effect of H_2O on controlling the aggregation of nanocrystals, the thermogravimetric analyses (TGA, Mettler Toledo SDTA851^e, atmosphere was O_2 50 mL/min, heating rate was 20 °C/min) of the aggregates with different particle size were conducted. Thermogravimetric/mass spectrometric measurement (TG/MS analysis, Netzsch STA449C/Balzers ThermoStar, atmosphere was air 20 mL/min, heating rate was 10 °C/min) was also applied to track the thermal degradation of the aggregates.

The dispersibility and particle size distribution of the nanocrystals and aggregates were characterized with a transmission electron microscope (TEM, JEM100-CXII). The oriented aggregation of the nanocrystals and the existence of mesopores in the particles were proved by the high-resolution transmission electron microscopy (HRTEM GEOL-2010) image and XRD patterns.

Results and Discussion

Synthesis and Characterization of the Intermediate Product. With the n-$C_6H_{13}OH$ solution of $Co(NO_3)_2\cdot 6H_2O$ refluxing at a reduced pressure, the boiling point of the solution continues increasing from 90 to 110 °C and the solution color turns purple. After removal of some n-$C_6H_{13}OH$ and cooling the solution to room temperature, a red solid is crystallized. As a d^7 metal ion, the stability of the octahedral Co^{2+} complexes such as $[Co(H_2O)_6]^{2+}$ are much smaller, and there are more tetrahedral complexes of Co^{2+} than for other transition metal ions.[31] For example, when $Co(NO_3)_2\cdot 6H_2O$ is heated, the hydration water will be eliminated.[31] The increasing of the boiling point of the solution indicates that the hydration water is gradually eliminated from the solution. And the color change might be the result of the coordination number decreasing of the center Co^{2+}, related to the elimination of hydration water.[31] The IR spectra similitude of the intermediate product and *n*-hexyl alcohol indicates no apparent δ_{HOH} mode of water at 1630 cm^{-1} is observed.[27,32] The bands at 1350, 1300, and 820 cm^{-1} are attributed to the adsorption of the coordinated NO_3^-,[27, 32] and the additional strong adsorption band at 1017 cm^{-1} might be due to the blue shift of C−O vibration band of *n*-hexyl alcohol commonly at 1050 cm^{-1}, probably resulting from the *n*-hexyl alcohol coordinating to Co^{2+} when water is eliminated and the solution cools to room temperature (Figure 2). The UV−visible spectra analysis proves that the Co^{2+} cation is hexacoordinated in *n*-hexanol solution. The ^{1}H NMR spectrum comparison of *n*-hexanol and intermediate product further proves $C_6H_{13}OH$ coordinating to Co^{2+} cation in $Co(NO_3)_2\cdot 7C_6H_{13}OH$ molecule. The intermediate product appears as a fine powder and has good solubility in many hydrocarbons. But a good single crystal could not be obtained to determine its crystal structure. All the peaks in its XRD patterns (Figure 2) give repeat distances of ca. 4.7°, indicating a pure lamellar crystalline phase and corresponding to the largest interplanar spacing of ca. 1.8 nm. The compositional analysis gives its chemical formula of $Co(NO_3)_2\cdot 7C_6H_{13}OH$. (The elemental analysis results: C, 56.58%; N, 3.14%; H, 10.16%; Co (by chemical titration), 6.40%.) According to this formula, the calculated values are C 56.17%, N 3.12%, H 10.91%, and Co 6.56%, which is consistent with the experiment results in the measurement error. On the basis of the above characterization, it is concluded that NO_3^- and $C_6H_{13}OH$ coordinate to Co^{2+}, forming a coordination octahedron, with which as building blocks a lamellar phase $Co(NO_3)_2\cdot 7C_6H_{13}OH$ with the largest interplanar spacing of about 1.8 nm forms.

Synthesis of Monodispersed Nanocrystals. This intermediate product is decomposed at a set tempera-

(31) (a) Cotton, F. A.; Wilkinson, G.; Murillo, C. A.; Bochmann, M. *Advanced Inorganic Chemistry Sixth Edition*; Wiley-Interscience: New York, 1999; part 3, p 817. (b) Xie, G.; Yu, L.; Liu, B. In *The Collection of Inorganic Chemistry*; Science Publishing House: Beijing, China, 1996; Vol. VIIII, p 302.

(32) (a) Fernandez, J. M.; Barriga, C.; Ulibarri, M. A.; Labajos, F. M.; Rives, V. *J. Mater. Chem.* **1994**, *4*, 1117. (b) Chisem, I. C.; Jones, W. *J. Mater. Chem.* **1994**, *4*, 1737.

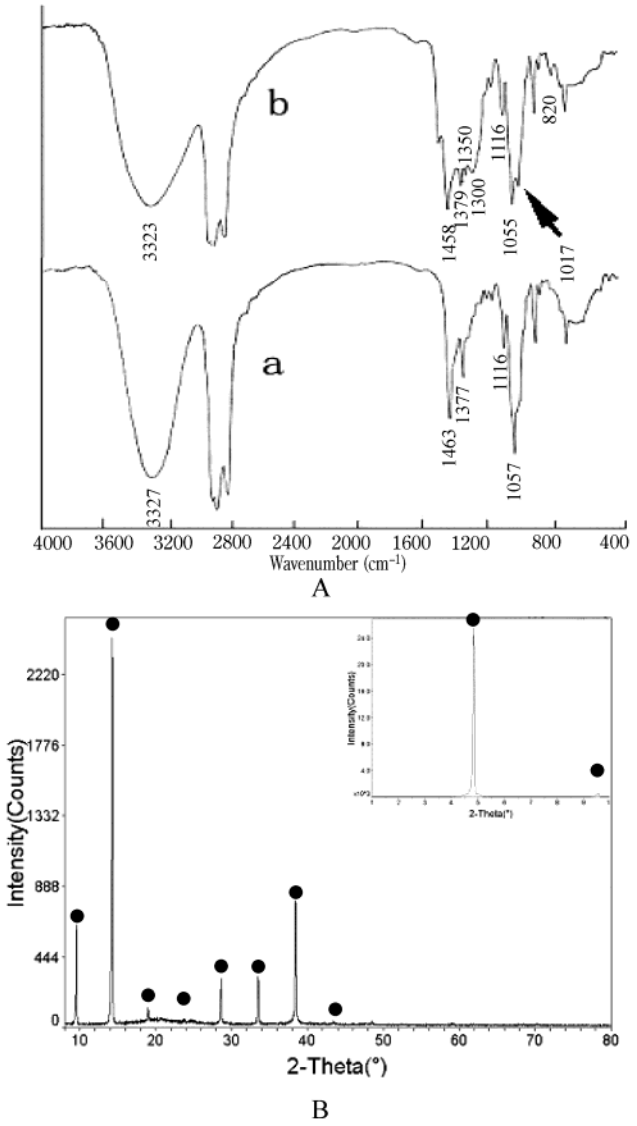

Figure 2. (A) IR spectra of (a) *n*-hexyl alcohol and (b) intermediate product and (B) the XRD pattern of the intermediate.

ture in n-$C_8H_{17}OH$ solution to give Co_3O_4 nanocrystals, which can disperse in cyclohexane to form a transparent solution. The TEM image (Figure 3) indicates that the Co_3O_4 nanoparticles with a diameter of 5 nm, which is consistent with that calculated from the XRD pattern (Figure 4a) with a Scherrer equation, have a narrow size distribution, and the inset lattice fringe image is indicative of their crystalline nature. The IR spectra (Figure 5) demonstrate the hybrid chemical nature of the nanocrystals with alcohols on the particle surface. The adsorption peaks at ca. 2900 and 1050 cm^{-1} attributed to the C−C and C−O vibrations prove that the long carbon chain alcohols are chemically bonded to the Co_3O_4 nanoparticles.

Nonagglomerated nanocrystals are of great importance for their future technology applications for their different properties from both bulk material and atom or molecular species. Moreover, they are also the building blocks in the self-assembly approach to construct nanostructured materials, and the synthesis is still a challenge, especially for the metal oxide nanocrystals. The surface hydroxyl is one of the dominant factors

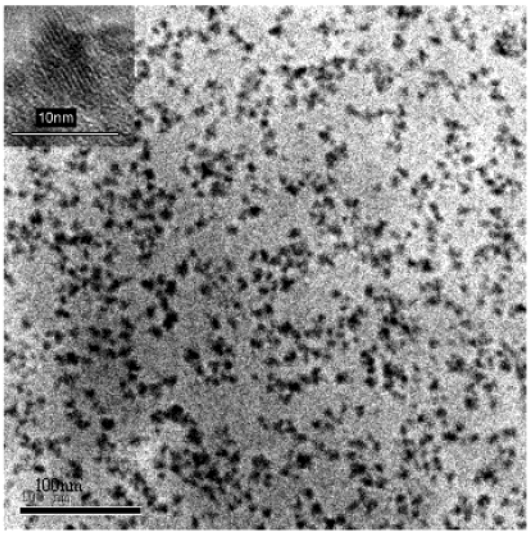

Figure 3. TEM image of the 5-nm nanocrystals.

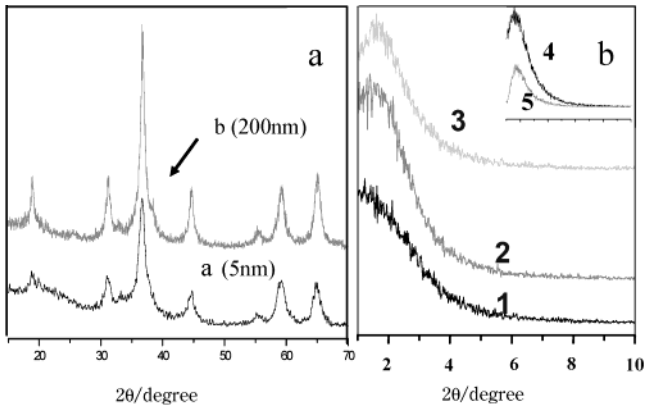

Figure 4. (a) XRD patterns of 5- and 200-nm particles (b) The low-angle XRD patterns of the mesoporous hybrids prepared in (1) *n*-hexyl alcohol, (2) *n*-octanol, (3) *n*-decanol, and the inset is that in *n*-decanol before (4) and after (5) solvothermal treatment.

resulting in the agglomeration of metal oxide nanocrystals. To obtain monodispersed oxide nanocrystals, a few nonhydrolytic processes through the thermodecomposition of metallorganics with the existence of capping agents are reported.[4] In the present process, the Co_3O_4 nanoparticles capped by the long carbon chain alcohol molecules appear monodispersible in hydrocarbons.

When heated to 120 °C, the red $Co(NO_3)_2{\cdot}7C_6H_{13}OH$ solution turns purple, and then black, accompanied by the formation of Co_3O_4 nanocrystals if the temperature continues up to 150 °C; simultaneously, brown NO_2 gas forms. The gas chromatography-mass spectrum analysis shows that, in the liquid reaction mixture, the total content of *n*-octanol (72%) and *n*-hexanol (16%) is about 90%, and the remanent content is some aldehydes usually existing in alcohol as impurities. Thus, on the basis of the above information, the decomposition mechanism of $Co(NO_3)_2{\cdot}7C_6H_{13}OH$ in alcohol solution can be expressed as follows:

$$3Co(NO_3)_2{\cdot}7C_6H_{13}OH \xrightarrow{150-180\ ^\circ C} Co_3O_4 + 6NO_2\uparrow + O_2\uparrow + 21C_6H_{13}OH$$

Thermodecomposition of cobalt salt, especially cobalt

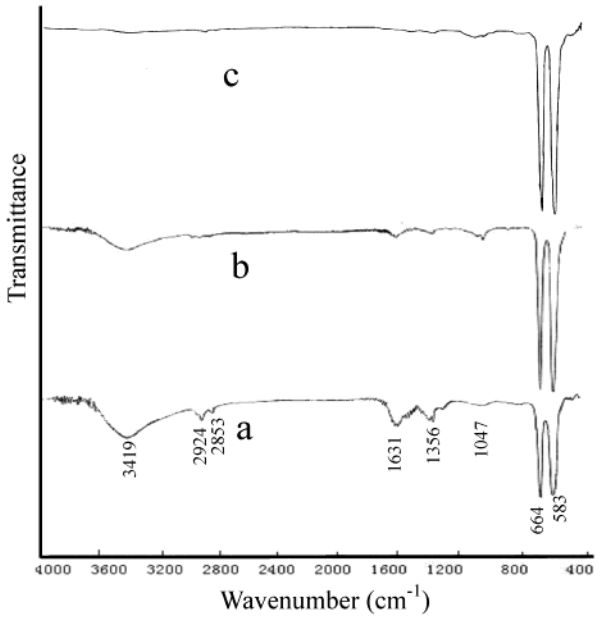

Figure 5. IR spectra of the aggregates: (a) the prepared particles, heated at (b) 300 °C and (c) 500 °C for 0.5 h in air.

nitrate, is the common method for preparation of Co_3O_4 due to the mild decomposition temperature of ca. 200 °C.[33] The cell size of Co_3O_4 from cobalt nitrate decomposition changes greatly with the variation of the reaction temperature and time, and many reasons have been proposed to explain the phenomenon.[33] Recently, it is found that the water from the starting salts is dissociatively accommodated in the product lattice, causing the cell size variation.[33e] Herein, the thermodecomposition of $Co(NO_3)_2 \cdot 7C_6H_{13}OH$ in nonaqueous solution may be more reproducible. On the other hand, as a promising catalyst, a big surface area for the spinel Co_3O_4 is usually required, which demands the preparation at a temperature as low as possible. For example, the cobalt hydrotalcite-like compounds are used to lower the decomposition temperature.[27] Compared with $Co(NO_3)_2 \cdot 6H_2O$, the decomposition of $Co(NO_3)_2 \cdot 7C_6H_{13}OH$ does not give the hydroxide or hydrous oxide intermediate and the synthetic temperature decreases by about 50 °C. The color change probably results from the coordination number decreasing due to the coordinated alcohols departure from Co^{2+}. This might give the NO_3^- anions a chance to sufficiently approach the Co^{2+} cations and partially oxidize Co^{2+} to Co^{3+}.

Control Synthesis of the Monodispersed Nanoparticles. A series of nanoparticles with a controlled size from 40 to 200 nm can be constructed based on the oriented aggregation of Co_3O_4 nanocrystals (i.e., the subsequent discussion). It is found that when the reaction temperature is raised or the reaction time is prolonged, the particle sizes increase, accompanied by the broadening of the size distribution. With the water content in the solvent increasing and keeping other reaction conditions unchanged, the particle size of the aggregates increases. When the molar ratio of H_2O to $Co(NO_3)_2 \cdot 7C_6H_{13}OH$ is 1.5, the 40-nm aggregates are produced. When the ratio is increased up to 5 and 12, the aggregate particle size increases to 90 and 200 nm, respectively. The diameters of the particles with standard deviation analyzed from TEM images are respectively 40 ± 5, 90 ± 5, and 200 ± 60 nm (Figure 6). The TEM characterizations indicate the aggregates can exist stably, keeping their shape and size unchanged in a series of hydrocarbons such as in normal octane, cyclohexane, and octanol.

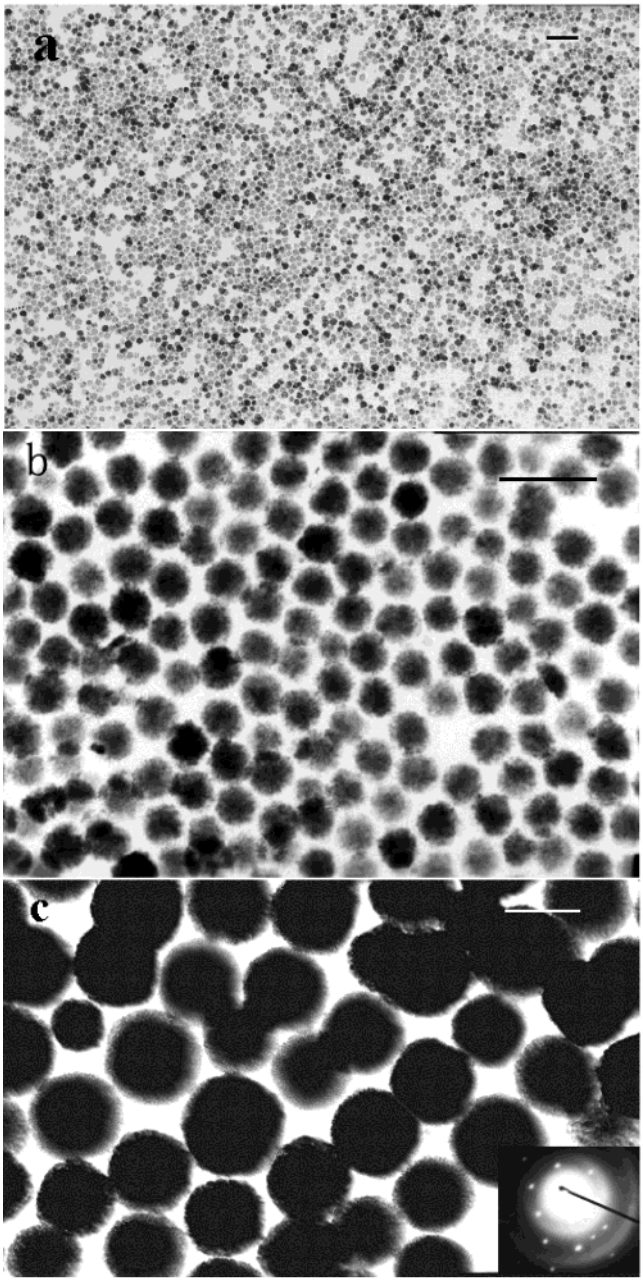

Figure 6. TEM images of (a) 40-, (b) 90-, and (c) 200-nm nanoparticles. The scale bar: 200 nm.

In an aqueous solution, the aggregation growth will initiate when the repulsive interactions, caused by the electrostatic or the steric hindrance between primary particles, are not large enough to block their access due to Brownian motion and van der Waals attraction. Adjusting the above parameters may provide control

(33) (a) Keely, W. M.; Maynov, H. W. *J. Chem. Eng. Data* **1963**, *8*, 297. (b) Garavaglia, R.; Mari, C. M.; Trasatti, S.; De Asmundis, C. *Surf. Technol.* **1983**, *19*, 197. (c) El Baydi, M.; Poillerat, G.; Rehspringer, J.-L.; Gautier, J. L.; Koening, J.-F.; Chartier, P. *J. Solid State Chem.* **1994**, *109*, 281. (d) Hill, R. J.; Craig, J. R.; Gibbs, G. V. *Phys. Chem. Mineral.* **1979**, *4*, 317. (e) Longhi, M.; Formaro, L. *J. Mater. Chem.* **2001**, *11*, 1228.

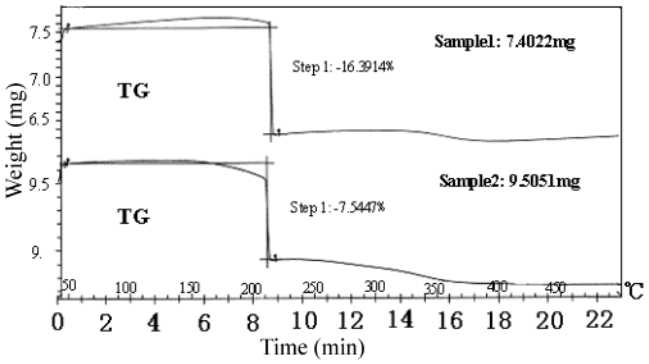

Figure 7. TG curves of the 40-nm (upper) and 200-nm (lower) particles.

over the aggregation process.[34] In the nonaqueous system, the designed addition of water provides a new, simpler method to prepare oxide nanoparticles with controlled size and narrow size distribution. This is quite different from the size-controlled synthesis of oxide and non-oxide nanoparticles in most former reports. In the method described herein, water provides surface hydroxyls that act as binders, making the nanocrystals aggregate. Because the water molecule coordination to metal ions is stronger than the alcohol molecule coordination, the coordinated alcohol molecules will be substituted when water is added into the reaction solution. With the formation of nanocrytals, the added water converts into surface hydroxyls, facilitating the nanocrystals' aggregation. It is reasonable to deduce that when other conditions such as the raw material concentration, reaction temperature, and time are kept unchanged, the different molar ratio of H_2O to $Co(NO_3)_2 \cdot 7C_6H_{13}OH$ will cause a different density of surface hydroxyls on the nanoparticle surface, which may be the direct reason for easy control over the particle size and size distribution during the aggregation process. The larger value of the surface hydroxyl density will lead to the formation of larger particles. The conclusion can be substantiated by the TG (Figure 7) and IR (Figure 5) analyses of the aggregates with different particle size. (The samples for the TG and IR measurements are first washed ultrasonically with cyclohexane and centrifuged three times and then dried at 120 °C in a vacuum for 0.5 h to eliminate the absorbed alcohols.) Both the TG curves of the 40- and 200-nm particles show the similar two-step weight loss. The first sharp weight loss is at ca. 210 °C and the second one is wider from 250 to 350 °C. The IR analysis proves that the first weight loss is mainly attributed to the elimination of *n*-hexanol on the nanocrystal surface based on the molar ratio of C to H of the TG/MS result, and the second one is due to the removal of surface hydroxyl.[35] With the aggregated particle size enlarged from 40 to 200 nm, the first step weight loss decreased from 16.39% to 7.54%, while the second one increased from 1.3% to 2.1%. The result reveals that there are many more alcohols and fewer hydroxyls in the smaller aggregates. Two small rises in the TG curve for the 40-nm particles respectively from 50 to 200 °C and from 210 to 270 °C appeared. Prior to the TG analysis, vacuum-drying at 120 °C for 0.5 h was applied for the samples. The absorption of O_2 on the particle surface occurred when TG analysis was carried out in an O_2 atmosphere, corresponding to the first rise in the TG curve from 50 to 200 °C. When the surface alcohols were eliminated as the temperature increased to 210 °C, the outmost Co^{2+} cations in the nanocrystals formerly bonded to the alcohols were denuded and consequently reacted with O_2, causing the second rise in the TG curve. TG/MS analysis is also conducted to identify the evolved gaseous products, which further proves the two weight losses in TG curves (Figure 7) corresponding respectively to the surface alcohols and the surface hydroxyls, and except for a spot of NO_2 gas, no other impurity exists on the aggregate surface.

Oriented Aggregation of the Nanocrystals. The high-magnification TEM image shown in Figure 8a indicates that the aggregates are constructed of 5-nm nanocrystals, and the wormlike nanopores with pore size of ca. 2 nm can be seen clearly, forming the special loose nanostructures. The selected area electron diffraction (SAED, Figure 8b) gives the [011] zone axis spots characteristic of a Co_3O_4 single crystal. The high-resolution transmission electron microscopy (HRTEM Figure 8c) shows a more compact particle image when the electron beam projects along the [011] direction than that that projects deviating the zone axis (Figure 8a). The parallel lattice fringes among almost all the primary building blocks and the grain boundaries (marked with white arrows) as well as the "dimples" and "crease" (marked with black arrows) in the HRTEM image (Figure 8c) can be seen clearly. All the above information confirm the perfectly oriented aggregation of nanocrystals,[16] and SAED spots, the fast Fourier transform (FFT), and invert fast Fourier transform (IFFT) images further confirm the oriented aggregation along the [011] direction.[36]

The low-angle XRD patterns of the larger aggregates (>200 nm) give a broad peak due to the ordered mesoporous structure (Figure 4b).[37] It is found that after solvothermal treatment in cyclohexane at 180 °C for 5 h, the ordered mesostructure is still kept and the characteristic diffraction peak shifts to the right a little (the inset in Figure 4b). However, this diffraction peak disappears after hydrothermal treatment at the same conditions, indicating the decreasing of the order. The electron diffraction ring of the particle whose low-angle diffraction peak disappears proves that the mesoporous structure is caused by the oriented aggregation of the Co_3O_4 nanocrystals. Further experiments demonstrate the mesostructure modulated through a selected alcohol as solvent. The longer the alcohol's carbon chain, the larger the 2θ of the low-angle XRD peaks, and the larger 2θ of the low-angle XRD peaks indicates the smaller *d* spacing of the mesostructure (Figure 4b); the correlation

(34) (a) Van Hyning, D. L.; Klemperer, W. G.; Zukoski, C. F. *Langmuir* **2001**, *17*, 3120. (b) Van Hyning, D. L.; Klemperer, W. G.; Zukoski, C. F. *Langmuir* **2001**, *17*, 3128.

(35) The IR spectrum of the as-prepared aggregates show the adsorption bands of *n*-octanol at 2900 and 1050 cm^{-1} and of surface hydroxyl at 3400 and 1630 cm^{-1}; after heat treatment at 300 °C for 0.5 h, the adsorption bands of the alcohols disappear; after heat treatment at 500 °C for 0.5 h, the adsorption bands of the hydroxyls also disappear.

(36) Joint Committee on Powder Diffraction Standards, International Centre for Diffraction Data, Card No. 43-1003, Swarthmore, PA, 1996.

(37) Kresge, C. T.; Leonowicz, M. E.; Roth, W. J.; Vartuli, J. C.; Beck, J. S. *Nature* **1992**, *359*, 710.

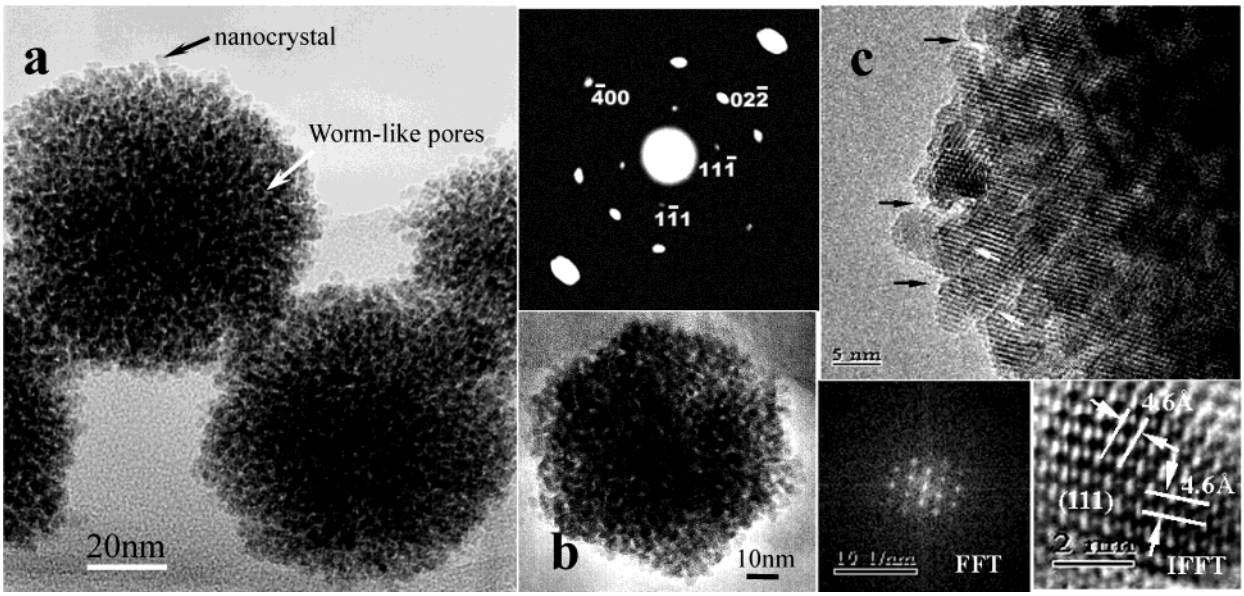

Figure 8. (a) High-magnification TEM image, (b) SAED pattern and the image when the electron beam projects along the [011] zone axis, and (c) HRTEM image with the FFT and IFFT images of the 90-nm particles.[36]

between the *d* spacing and length of the alcohol carbon chain is not yet clear.

In former reports, oriented aggregation is mainly investigated as one of the important crystal growth mechanisms, especially in aqueous solutions. It has been proposed that only the ligand-free primary nanoparticles could carry out oriented aggregation, and the oriented attachment of preformed quasi-spherical ZnO nanoparticles to single-crystalline nanorods may be a good example. While the 5-nm nanocrystals capped with long carbon chain alcohols in nonaqueous conditions can also form a perfectly oriented aggregate, a mesoporous-like nanostructure forms. The main driving force for oriented aggregation of the nanocrystals is currently attributed to the tendency to decrease the high surface energy. And in aqueous solutions, through the rotations of the primary nanocrystals caused by various interactions such as Brownian motion, and the short-range interactions between adjacent surfaces, oriented aggregation can be realized.[14] If other unwished interactions such as the bonding of the nanocrystals with surfactant ligands exist, oriented aggregation will probably be inhibited or confined in small regions in a large polycrystalline material.[14] While the long carbon chains on the surface of the 5-nm nanocrystals in the nonaqueous system could not provide any unwished interactions, they might instead make the aggregation rate a little slower than in aqueous solutions and, like a lubricant, make the rotation of adjacent particles more free, finally resulting in the perfect oriented aggregation. The parallel experiments of the decomposition reaction respectively using the absolute ethanol and *n*-octanol as the solvent carried out at the same solvothermal conditions result in the larger polycrystalline particles and the monodispersed nanoparticles with the oriented aggregation structures. We feel that this confirms our considerations. Another interesting thing is that the particle size calculation based on the XRD patterns is much smaller than that given by the TEM images (see Figure 4a), indicating the crystal growth may be greatly inhibited. The capping effect of the long carbon chain of the alcohols might be one reason for the prevention of their complete aggregating growth, and the difficult mass transport of the ions of oxide in a nonaqueous system might be another reason for the weakening of the coarsening growth.

Conclusion

Through the reaction of $Co(NO_3)_2 \cdot 6H_2O$ with *n*-hexyl alcohol, the intermediate product $Co(NO_3)_2 \cdot 7C_6H_{13}OH$ is obtained. The thermal decomposition of $Co(NO_3)_2 \cdot 7C_6H_{13}OH$ in the long carbon chain alcohols results in the formation of the uniform monodispersed Co_3O_4 nanoparticles with the size from 5 to 200 nm. The as-prepared particles are constructed through the oriented aggregation of the primary 5-nm nanocrystals and the size control is realized by the designed addition of water into the reaction system. The oriented aggregation gives a mesoporous-like structure of the particles with ca. 2-nm wormlike pores.

The designed addition of water into the nonaqueous solution offers a novel route for the controlled synthesis of metal oxide nanoparticles and is quite different from most former reports. The binder effect of water molecules on the controlled aggregation of metal oxide nanocrystals is emphasized.

Aggregation in nonaqueous conditions is kinetically different from that in electrolytic solutions, causing perfect oriented aggregation of the primary building blocks. The capping effect of the surface alcohols results in the formation of the mesoporous-like structure by oriented aggregation.

Acknowledgment. This work was supported by the Key Technologies R & D Program of P. R. China, and Shandong Foundation for Innovation. The authors thank Prof. Wenxing Zhang and Jimao Lin for their assistance on explaining the IR and NMR spectra and Dr. Augustus Dunning for editing the English of the manuscript.

Supporting Information Available: Additional experimental details and figures (PDF). This material is available free of charge via the Internet at http://pubs.acs.org.

CM0303033